AD_____

Award Number: W81XWH-11-1-0426

TITLE: Role of IKKalpha and STAT3 in the Emergence of Castration-Resistant Prostate Cancer

PRINCIPAL INVESTIGATOR: : Massimo Ammirante

CONTRACTING ORGANIZATION:
University of California, San Diego

La Jolla, CA 92093-0723

REPORT DATE: June 2013

TYPE OF REPORT: Annual Summary

PREPARED FOR: U.S. Army Medical Research and Materiel Command
Fort Detrick, Maryland 21702-5012

REPORT DOCUMENTATION PAGE

Form Approved
OMB No. 0704-0188

1. REPORT DATE	2. REPORT TYPE	3. DATES COVERED
June 2013	Annual Summary	1 June 2011 – 31 May 2013

4. TITLE AND SUBTITLE

Role of IKKalpha and STAT3 in the Emergence of Castration-Resistant Prostate Cancer

5a. CONTRACT NUMBER
W81XWH-11-1-0426

5b. GRANT NUMBER
W81XWH-11-1-0426

5c. PROGRAM ELEMENT NUMBER

5d. PROJECT NUMBER

5e. TASK NUMBER

5f. WORK UNIT NUMBER

6. AUTHOR(S)
Massimo Ammirante

E-Mail: mammirante@ucsd.edu

7. PERFORMING ORGANIZATION NAME(S) AND ADDRESS(ES)
The Regents of the Univ. of Calif., U.C. San Diego
La Jolla, CA 92093-0723

8. PERFORMING ORGANIZATION REPORT NUMBER

9. SPONSORING / MONITORING AGENCY NAME(S) AND ADDRESS(ES)
U.S. Army Medical Research and Materiel Command

Fort Detrick, Maryland 21702-5012

10. SPONSOR/MONITOR'S ACRONYM(S)

11. SPONSOR/MONITOR'S REPORT NUMBER(S)

12. DISTRIBUTION / AVAILABILITY STATEMENT
Approved for Public Release; Distribution Unlimited

13. SUPPLEMENTARY NOTES

14. ABSTRACT

A major complication of androgen ablation therapy for prostate cancer (PC) is the development of castration resistant PC (CRPC) that is more aggressive and more prone to metastatic spread. We previously demonstrated that CRPC development is accelerated by infiltrating B cells that are recruited into regressing androgen-deprived tumors by the chemokine CXCL13, whose expression was found to correlate with clinical severity in human PC. Here we describe how androgen ablation leads to CXCL13 expression. In both subcutaneously transplanted tumors and spontaneous PC in mice CXCL13 is expressed by tumor-associated myofibroblasts that are activated upon androgen ablation. Myofibrolast activation and CXCL13 expression are also induced upon castration within the normal prostate and CXCL13 and myofibroblast markers are co-expressed in human PC. Androgen ablation results in appearance of hypoxic regions and nuclear HIF-1α within the regressing tumors and hypoxia leads to myofibroblast activation and CXCL13 induction in a HIF-1α-dependent manner. Myofibroblast activation and CXCL13 induction are also dependent on signaling by TGFβ family members, whose expression induced in response to hypoxia and androgen ablation. Immunodepletion of myofibroblasts or inhibition of TGFβ signaling retard the development of CRPC in transplanted tumors and block it completely in the TRAMP model of spontaneous PC.

15. SUBJECT TERMS
hypoxia, myofibroblasts, castration resistant prostate cancer, TGF-beta

16. SECURITY CLASSIFICATION OF:			17. LIMITATION OF ABSTRACT	18. NUMBER OF PAGES	19a. NAME OF RESPONSIBLE PERSON
a. REPORT	b. ABSTRACT	c. THIS PAGE			USAMRMC
U	U	U	UU	21	19b. TELEPHONE NUMBER *(include area code)*

Table of Contents

INTRODUCTION:

I recently found that androgen ablation therapy triggers an inflammatory response that is likely to be caused by the death of androgen-dependent CaP cells (Ammirante et al., 2010). The inflammatory response results in infiltration in the tumor remnant with a variety of lymphocytes, including B cells that express lymphotoxin (LT), a member of the TNF family. LT producing B cells lead to the activation of IKKα and STAT3 in surviving CaP cells and thereby enhance the ability to survive and continue to proliferate in the absence of androgens. An unknown component of the mechanism that promotes the emergence of CR-CaP is the cell type that produces the proinflammatory chemokine CXCL13 in response to androgen ablation. CXCL13 is the chemokine that leads to the recruitment of LT-producing B cells into the tumor remnant, a process that is critical for IKKα and STAT3 activation in CaP cells and the emergence of CR-CaP. Once the CXCL13-producing cells will be identified their role in emergence of CR-CaP will be examined. This research will result in identification of new therapeutic targets for prevention of CR-CaP. For instance, we may be able to delay the emergence of CR-CaP by inhibiting the induction of CXCL13. These approaches may also be useful for inhibition of metastatic progression of CaP.

BODY:

Using the Myc-CaP transplantable model of androgen-dependent mouse PC (Watson et al., 2005) we examined how androgen ablation leads to induction of CXCL13 expression, which is critical for recruitment of B cells into the tumor remnants and accelerated evolution of CRPC (Ammirante et al., 2010). Myc-CaP cells were inoculated subcutaneously (s.c.) into 6 weeks old FVB/N males and when the tumors had reached 1 cm^3 in size the mice were castrated to deprive the tumors of androgens. Following castration, we found that many myofibroblasts positive for smooth muscle actin (SMA) were present within the tumors remnants and that expression of CXCL13 mRNA was strongly elevated (Fig 1A). To identify which cells express CXCL13 we isolated different cell types from the androgen-deprived tumors using cell fractionation. Expression of CXCL13 and fibroblast activation protein (FAP), an enzyme that serves as another myofibroblast marker (Chen et al., 2009), were detected only in the fibroblast fraction and not in the epithelial fraction prepared 1 week after castration (Fig 2A). The $CD11b^+$ and $CD11c^+$ fractions of the tumors were also negative for expression of CXCL13 and FAP (Fig 2B). To deplete the myofibroblasts in the androgen-deprived tumor stroma we orally administered a DNA vaccine encoding FAP that is specifically delivered to secondary lymphoid tissues by a non-infectious, attenuated, live *Salmonella typhimurium* vector (Loeffler et al., 2006). This vaccine strategy was shown to induce a strong cytotoxic T cell response that results in specific killing of fibroblasts within the tumor stroma of mammary cancer (Loeffler et al., 2006). Ablation of FAP-expressing cells using this vaccine also resulted in the disappearance of myofibroblasts that are positive for CXCL13 in the stroma of androgen-deprived Myc-CaP tumors (Fig 1B). Importantly, the immune-mediated ablation of FAP-positive cells was as effective as the genetic or antibody-mediated ablation of B cells (Ammirante et al., 2010) in retarding the evolution of CRPC after castration (Fig 1C). In addition, the ablation of FAP-expressing cells led to a marked reduction in the infiltration of T, B and dendritic cells into the tumor remnants after castration, but had a little effect on the infiltration of macrophages (Fig 2C). FAP vaccination also reduced the expression of several other chemokines in addition to CXCL13 (Fig 2D). Consistent with its ability to block B cell infiltration into the androgen-deprived tumors, the FAP vaccine also prevented the nuclear translocation of IKKα in cancer cells (Fig 1D). These results suggest that after castration CXCL13 is mainly expressed by activated myofibroblasts in the tumor microenvironment.

We also found that androgen ablation led to increased expression of TGFβ family members in the tumor remnants, that peaked at 4 days after castration (Fig 3A). Since TGFβ is involved in fibroblast activation (Gabbiani, 2003), we blocked TGFβ signaling with a specific inhibitor of the TGFβ type I receptor (TGFβ RI) also known as activin receptor-like kinases ALK5 and ALK4 and ALK7, SB-431542 (Inman et al., 2002). Inhibition of TGFβ RI signaling prevented activation of myofibroblasts (Fig 4A) as well as nuclear translocation of SMAD2/3 (Fig 3B), infiltration of B cells (Fig 3C), induction of CXCL13-expressing myofibroblasts (Fig 3C,D) and nuclear translocation of IKKα (Fig 3E). SB-431542 treatment also delayed the re-growth of CRPC (Fig 3F). In addition, SB-431542 treatment reduced the expression of several other

chemokine mRNAs within the tumors (Fig 4B) and inhibited the recruitment of B, T, NK, dendritic cells and macrophages (Fig 4C). After castration, FAP expression peaked at day 4, whereas CXCL13 induction and B recruitment started peaking at day 6; all of these events were inhibited by SB-431542 (Fig 4D). SB-431542 also inhibited castration-induced myofibroblast activation in the normal prostate, the only other tissue in which androgen ablation led to myofibroblast activation (Fig 4E).

The main source of TGFβ in Myc-CaP androgen-deprived tumors is also the fibroblast fraction, rather then the epithelial or the myeloid $CD11b^+$ or $CD11c^+$ cell populations (Fig 5A,B). After castration there is also an increase in the expression of mRNAs coding for the 38 kDa glycoprotein (GP38), another myofibroblast marker (Roozendaal and Mebius, 2011), connective tissue growth factor (CTGF) and insulin-like growth factor 1 (IGF-1), particularly at 4 days after castration for GP38 and CTGF mRNAs (Fig 6A). Ablation of FAP^+ cells with the FAP vaccine significantly reduced the castration-elicited induction of IGF-1, CTGF and TGFβ (Fig 5C), confirming that three growth factors are expressed by FAP^+ myofibroblasts. Previous studies have shown that one function of CTGF is to potentiate TGFβ signaling (Grotendorst, 1997). Stimulation of inactive fibroblasts isolated from Myc-CaP tumors of sham operated mice with CTGF plus TGFβ led to induction of FAP, α-SMA and CXCL13 mRNAs, but treatment of these cells with $TGF\beta_1$ or CTGF alone was ineffective (Fig 7A). Fibroblasts that were isolated from Myc-Cap tumors 1 week after castration showed as expected elevated expression of FAP and α-SMA, but these cells did not retain CXCL13 expression after isolation (Fig 7A). Nonetheless, in these cells $TGF\beta_1$ alone was sufficient to induce CXCL13 mRNA expression. FAP and α-SMA but not CXCL13 were also induced in fibroblasts isolated from sham mice upon treatment with either IGF-1 alone or IGF-1 plus CTGF but not CTGF alone (Fig 6B). In fibroblasts isolated from androgen-deprived tumors, which already expressed FAP and α-SMA mRNAs, CXCL13 mRNA expression was also induced upon IGF-1 treatment. However, IGF-1 is unlikely to have a critical role in CXCL13 induction in androgen-deprived tumors because its expression is increased only at 7 days after castration whereas myofibroblasts are already activated after 4 days (Fig 6A) and CXCL13 is expressed at maximal levels at 6 days post-castration (Fig 4D).

Since castration results in injury of androgen-dependent tissues, and after tissue injury the ensuing tissue hypoxia is thought to be one of the main factors that triggers wound healing (Guo and Dipietro, 2010), we decided to study the role of hypoxia in fibroblast activation and CXCL13 induction. The culturing of inactive fibroblasts isolated from Myc-CaP tumors of non-castrated mice under hypoxic conditions converted the fibroblasts into myofibroblasts, as judged by FAP and α-SMA expression and led to induction of CXCL13 CTGF, IGF-1 and TGFβ mRNAs (Fig 7B). Hypoxia also led to induction of CTGF, IGF-1, TGFβ and CXCL13 mRNAs in fibroblasts isolated from Myc-CaP tumors from castrated mice, although these fibroblasts were already activated as indicated by FAP and α-SMA expression (Fig 7B).

Importantly 2 days after surgical castration, hypoxic areas appeared within the tumors along with nuclear translocation of HIF-1α in both cancer cells and stromal cells (Fig 7C). The hypoxic response may be caused by disruption of tumoral blood vessels, which starts the hypoxic response at 2 days after castration, based on staining with a CD34 antibody (Fig 8A). Curiously, CD-34 expressing cells re-appear 8 days after castration, a time point that precedes tumor regrowth and follows the infiltration of the androgen-deprived tumors with immune and inflammatory cells (Ammirante et al., 2010). Notably, the $CD34^+$ cells that re-appear at 8 days after castration are not as tightly organized as the $CD34^+$ cells that reside within the tumors prior to castration (Fig 8A). Deletion of HIF-1α in fibroblasts isolated from *Hif-1α*$^{F/F}$ mice induced by expression of *Cre recombinase* (Ryan et al., 1998) prevented their hypoxia-induced conversion into myofibroblasts (Fig 8B). Induction of CTGF, IGF-1 and TGFβ mRNAs under hypoxic conditions was also dependent on HIF-1α (Fig 8C). CTGF and $TGF\beta_1$, $TGF\beta_2$ and $TGF\beta_3$ were previously described as HIF-1a regulated genes (Basu et al., 2011; Higgins et al., 2004; Schaffer et al., 2003; Zhang et al., 2003).

Similarly to its effects in s.c. Myc-CaP tumors, castration also led to induction of inflammatory cytokines, including LTα, LTβ and IL-6, CXCL13, TGFβ, immune infiltration and myofibroblast activation in the normal prostate, which is an androgen-dependent organ (Fig 9A-C). Similar findings were obtained in the SV40 T antigen-induced PC model, the TRAMP mouse (Greenberg et al., 1995). In particular, we observed induction of CXCL13, LTα, LTβ and TGFβ mRNAs, myofibroblast activation and B cell infiltration at 7 weeks after castration of TRAMP mice (Fig 9D,E). The effect of myofibroblast ablation using the FAP vaccine in TRAMP

mice was even more striking then in the Myc-CaP model. Almost no tumor tissue remained at 7 weeks after castration in TRAMP mice that were vaccinated with the FAP vector (Fig 9F). In addition to almost complete myofibroblast ablation (Fig 10A,B), FAP-vaccinated TRAMP mice exhibited more apoptotic cell death within the prostate tumors after castration relative to castrated mice that received the control TOPO vaccine (Fig 10C).

We also examined whether the human PC microenvironment contains fibroblasts that express CXCL13. Using specimens of different types of human prostate tissue we found that nuclear SMAD2/3 and FAP, CXCL13 and FAP and nuclear HIF-1α and FAP were co-localized in malignant prostate tissue, but not in normal prostate tissue or benign prostatic hyperplasia (Fig 11A-C). We also found that CXCL13 and FAP are co-localized in a transplant model in which primary human PC cells were xenotransplanted into mice along with human tumor stroma (Fig 11C).

KEY RESEARCH ACCOMPLISHMENTS

hypoxia activates myofibroblasts, TGF-β activates myofibrobasts, CXCL13 is expressed by myofibroblasts.

REPORTABLE OUTCOMES

AACR meeting: Tumor Immunology (Dec 2-5 2012, Miami) presentation:

Myofibroblasts activated upon tissue injury and hypoxia promote development of castration-resistant prostate cancer

Manuscript: *in preparation*

CONCLUSION

The results obtained suggest that CAFs may serve as therapeutic targets whose ablation or inhibition may improve the outcome of androgen ablation therapy. Using a previously described vaccine that leads to T cell-mediated elimination of myofibroblasts that express FAP (Loeffler et al., 2006) we have succeeded in preventing CXCL13 expression and B cell recruitment into s.c. Myc-Cap tumors subjected to androgen ablation. This resulted in a substantial 3 weeks delay in the emergence of CRPC. An even greater effect was seen in FAP vaccinated TRAMP mice in which CRPC development appears to have been totally blocked. However, while the FAP vaccine underscored the importance of targeting CAF as a way to improve the outcome of more conventional cancer therapies, including genotoxic chemotherapy (Sun et al., 2012), it is unlikely to be practical due to several reasons. Fist and foremost, activated FAP^+ myofibroblasts play an essential role in wound healing response, being responsible for collagen production, ECM deposition and formation of scar tissue (Li and Wang, 2011) Second, FAP ablation experiments have demonstrated that FAP^+ cells have important tissue protecting function because they either suppress the production of TNF-α and IFN-γ, or they attenuate cellular responses to these cytokines (Kraman et al., 2010). Third, FAP^+ myofibroblasts are closely related to lymphoid tissue stromal cells which are important for proper immune functions (Peduto et al., 2009). Thus a more practical approach would entail the specific and selective targeting of CAFs without elimination of all myofibroblasts. An even better approach would be to target the production of CAF-produced factors such as CXCL13 (Ammirante et al., 2010) and WNT16B (Sun et al., 2012) which mediated some of the CAF generated effects on tumor recurrence and resistance to therapy. The results obtained also show that fibroblasts are activated by castration-induced hypoxia in an autocrine way through the production of TGF-β, which induces the expression of CXCL13. The inhibition of TGFβ or the development or the use of neutralizing antibodies against CXCL13 could be used as another possible therapy to delay the emergence of CR-CaP.

REFERENCES

Ammirante, M., Luo, J., Grivennikov, S., Nedospasov, S. A., and Karin, M. (2010). B cell–derived lymphotoxin promotes castration-resistant prostate cancer. Nature *464*, 302-305.

Basu, R. K., Hubchak, S., Hayashida, T., Runyan, C. E., Schumacker, P. T., and Schnaper, H. W. (2011). Interdependence of HIF-1alpha and TGF-beta/Smad3 signaling in normoxic and hypoxic renal epithelial cell collagen expression. American journal of physiology Renal physiology *300*, F898-905.

Chen, H., Yang, W. W., Wen, Q. T., Xu, L., and Chen, M. (2009). TGF-beta induces fibroblast activation protein expression; fibroblast activation protein expression increases the proliferation, adhesion, and migration of HO-8910PM [corrected]. Experimental and molecular pathology *87*, 189-194.
Gabbiani, G. (2003). The myofibroblast in wound healing and fibrocontractive diseases. The Journal of pathology *200*, 500-503.
Greenberg, N. M., DeMayo, F., Finegold, M. J., Medina, D., Tilley, W. D., Aspinall, J. O., Cunha, G. R., Donjacour, A. A., Matusik, R. J., and Rosen, J. M. (1995). Prostate cancer in a transgenic mouse. Proc Natl Acad Sci U S A *92*, 3439-3443.
Grotendorst, G. R. (1997). Connective tissue growth factor: a mediator of TGF-beta action on fibroblasts. Cytokine & growth factor reviews *8*, 171-179.
Guo, S., and Dipietro, L. A. (2010). Factors affecting wound healing. Journal of dental research *89*, 219-229.
Higgins, D. F., Biju, M. P., Akai, Y., Wutz, A., Johnson, R. S., and Haase, V. H. (2004). Hypoxic induction of Ctgf is directly mediated by Hif-1. American journal of physiology Renal physiology *287*, F1223-1232.
Inman, G. J., Nicolas, F. J., Callahan, J. F., Harling, J. D., Gaster, L. M., Reith, A. D., Laping, N. J., and Hill, C. S. (2002). SB-431542 is a potent and specific inhibitor of transforming growth factor-beta superfamily type I activin receptor-like kinase (ALK) receptors ALK4, ALK5, and ALK7. Molecular pharmacology *62*, 65-74.
Kraman, M., Bambrough, P. J., Arnold, J. N., Roberts, E. W., Magiera, L., Jones, J. O., Gopinathan, A., Tuveson, D. A., and Fearon, D. T. (2010). Suppression of antitumor immunity by stromal cells expressing fibroblast activation protein-alpha. Science *330*, 827-830.
Li, B., and Wang, J. H. (2011). Fibroblasts and myofibroblasts in wound healing: force generation and measurement. Journal of tissue viability *20*, 108-120.
Loeffler, M., Kruger, J. A., Niethammer, A. G., and Reisfeld, R. A. (2006). Targeting tumor-associated fibroblasts improves cancer chemotherapy by increasing intratumoral drug uptake. J Clin Invest *116*, 1955-1962.
Peduto, L., Dulauroy, S., Lochner, M., Spath, G. F., Morales, M. A., Cumano, A., and Eberl, G. (2009). Inflammation recapitulates the ontogeny of lymphoid stromal cells. J Immunol *182*, 5789-5799.
Roozendaal, R., and Mebius, R. E. (2011). Stromal cell-immune cell interactions. Annual review of immunology *29*, 23-43.
Ryan, H. E., Lo, J., and Johnson, R. S. (1998). HIF-1 alpha is required for solid tumor formation and embryonic vascularization. The EMBO journal *17*, 3005-3015.
Schaffer, L., Scheid, A., Spielmann, P., Breymann, C., Zimmermann, R., Meuli, M., Gassmann, M., Marti, H. H., and Wenger, R. H. (2003). Oxygen-regulated expression of TGF-beta 3, a growth factor involved in trophoblast differentiation. Placenta *24*, 941-950.
Sun, Y., Campisi, J., Higano, C., Beer, T. M., Porter, P., Coleman, I., True, L., and Nelson, P. S. (2012). Treatment-induced damage to the tumor microenvironment promotes prostate cancer therapy resistance through WNT16B. Nature medicine *18*, 1359-1368.
Watson, P. A., Ellwood-Yen, K., King, J. C., Wongvipat, J., Lebeau, M. M., and Sawyers, C. L. (2005). Context-dependent hormone-refractory progression revealed through characterization of a novel murine prostate cancer cell line. Cancer Res *65*, 11565-11571.
Zhang, H., Akman, H. O., Smith, E. L., Zhao, J., Murphy-Ullrich, J. E., and Batuman, O. A. (2003). Cellular response to hypoxia involves signaling via Smad proteins. Blood *101*, 2253-2260.

Legend to the Figures

Figure 1: A. Six weeks old FVB/N male mice (n=10) were s.c. inoculated with Myc-CaP cells. When the tumors reached 1000 mm^3, mice were castrated or sham operated. Tumors were analyzed one week later for presence of α-SMA by immunohistochemistry (IHC) and for expression of CXCL13 mRNA by *in situ* hybridization (ISH) (Magnification: 200X). **B.** Six-weeks old male FVB/N mice (n=10 per group) were vaccinated three times with 10^8 CFU of TOPO or FAP vaccines every 5 days. Myc-CaP tumors were established as above. Three days before castration the mice received another dose of either vaccine. One week after castration tumors were collected, paraffin-embedded, sectioned and analyzed by IHC with α-SMA and CXCL13 antibodies (Magnification: 200X). **C.** FVB/N males (n=10 per group) were vaccinated and Myc-CaP tumors were established as described above. Tumor volume was measured every 2-3 days after castration. Results are expressed as means ± s.e.m.. **D.** Tumors collected 1 week after castration as in B, were analyzed for nuclear IKKα by IHC (Magnification: 200X).

Figure 2: **A, B.** FVB/N mice (n=10 per group) bearing Myc-CaP tumors were castrated or sham operated and sacrificed 1 week later. Tumors were removed, digested and the fibroblast (Fib), epithelial (Epi) (A), $CD11b^+$ and $CD11c^+$ cell fractions (B) were isolated, total RNA was extracted and CXCL13 and FAP (A) or CXL13 (B) mRNAs were quantitated by Q-PCR and normalized to cyclophilin A mRNA. Results are averages ± s.d.. **C-D.** FVB/N mice were vaccinated with TOPO and FAP vaccines and Myc-CaP tumors were established as described in Fig. 1B. One week after castration tumors were collected, total RNA was isolated and expression of the indicated mRNAs was quantitated by Q-PCR as above. Results are averages ± s.d..

Figure 3: A. Myc-CaP tumors (n=10) were established as in Fig. 1A and tumors were collected either after sham operation (7 days) or at the indicated days after castration (C). Total RNA was isolated and TGFβ1, TGFβ2 and TGFβ3 mRNAs were quantitated by Q-PCR and normalized to the amount of cyclophilin A mRNA. Results are averages ± s.d.. **B-E.** FVB/N mice bearing Myc-CaP tumors were castrated. Starting one day before castration, the mice (n=10 per group) were injected daily with vehicle or SB-431542 (0.2 mg/mouse; 10 mg/kg), a TGFβ RI (ALK5) inhibitor. Tumors were collected 1 week after castration and analyzed by IHC for α-SMA and nuclear SMAD2/3 (B, Magnification: 400X), α-SMA and CXCL13 (D, Magnification: 200X) and IKKα (E, Magnification: 200X) or subjected to RNA extraction and Q-PCR analysis of the indicated mRNAs (C, results are averages ± s.d.). **F.** Tumors were established and the mice were treated with SB-431542 or vehicle as above. Tumor volume was measured every 2-3 days. Results are expressed as means ± s.e.m.. P values >0.05 were considered non-significant (ns), 0.01 to 0.05 were considered significant (*), 0.001 to 0.01 were considered very significant (**) and < 0.001 were considered highly significant (***).

Figure 4: FVB/N mice (n=10 per experiment) bearing Myc-CaP tumors were castrated or sham operated and i.p. injected with SB-431542 or vehicle as described in Figure 3B. **A.** Tumors were collected 1 week after the operation, paraffin-embedded, sectioned and analyzed for α-SMA expression by IHC (Magnification: 200X). **B**, **C.** Tumors were

collected 1 week after castration, RNA was extracted and expression of the indicated mRNAs was quantitated by Q-PCR as above. Results are averages ± s.d.. **D.** Tumors were collected at the indicated time points and the expression of the indicated mRNAs was quantitated as above. Results are averages ± s.d.. **E.** Tumors, liver, lungs, kidneys and prostates were collected from FVB/N mice treated as above, total RNA was isolated one week after castration and α-SMA mRNA expression was quantitated as above. Results are averages ± s.d..

Figure 5: A, B. FVB/N mice (n=10) bearing Myc-CaP tumors were sham operated or castrated and tumors were collected 1 week later. Fibroblasts (Fib), epithelial (Epi), $CD11b^+$ and $CD11c^+$ cells were isolated from the tumors, total RNA was extracted and TGFβ1, TGFβ2 and TGFβ3 mRNAs were quantitated by Q-PCR and normalized to cyclophilin A mRNA. Results are averages ± s.d.. **C.** FVB/N mice were vaccinated with TOPO or FAP vaccines as in Fig. 1B and Myc-CaP tumors were established. One week after castration tumors were collected, total RNA was isolated and expression of the indicated mRNAs was quantitated and normalized to that of cyclophilin A mRNA. Results are averages ± s.d..

Figure 6: Myc-CaP tumors (n=10) were established in 6 weeks old FVB/N males that were castrated or sham operated. **A.** Tumors were collected at the indicated time points after operation, total RNA was isolated and expression of the indicated mRNAs was quantitated and normalized to that of cyclophilin A mRNA. Results are averages ± s.d.. **B**. Fibroblasts isolated from tumors of sham operated or castrated mice were cultured for 4 days and incubated for 6 hrs with either CTGF (50 ng/ml) or IGF-1 (10 ng/ml) alone or with CTGF plus IGF-1. FAP and α-SMA mRNA expression was quantitated as above**.** Results are averages ± s.d..

Figure 7: A. Fibroblasts were purified from Myc-CaP tumors 1 week after sham operation or castration (n=10 per group). The isolated cells were plated and stimulated for 24 hrs with $TGF\beta_1$ (10 ng/ml), CTGF (50 ng/ml) or $TGF\beta_1$ plus CTGF. RNA was isolated and expression of the indicated genes was analyzed as above. Results are averages ± s.d.. **B.** Fibroblasts were isolated as above from Myc-CaP tumors 1 week after castration or sham operation. The cells were cultured either in a standard incubator or a hypoxic chamber for 24 hrs. Total RNA was isolated and expression of the indicated mRNAs was quantitated. Results are averages ± s.d.. **C.** FVB/N mice bearing Myc-CaP tumors were castrated and tumors were collected at the indicated times after castration. For hypoxia analysis mice were i.p. injected 90 min before sacrifice with 60 mg/kg of pimonidazole hydrochloride (Hypoxiprobe-1). Tumors were removed, fixed, paraffin embedded, sectioned and subjected to IHC with hypoxiprobe or HIF-1α antibodies (Magnification: 200X). The arrows indicate hypoxic areas and cells with nuclear HIF-1α.

Figure 8: **A.** FVB/N mice bearing Myc-CaP tumors were castrated or sham operated and tumors were collected at the indicated time points after operation and stained for CD34 by IHC (Magnification: 200X)**. B.** Tumor associated fibroblasts were purified from *Hif-1α*$^{F/F}$ mice bearing Myc-CaP tumors, plated and infected with Adenovirus-Cre (Ad-Cre) or Adenovirus-GFP (Ad-GFP) and incubated in either a normal cell incubator or an

hypoxic chamber for 24 hrs. Total RNA was isolated and expression of the indicated mRNAs was quantitated and normalized to that of cyclophilin A. Results are averages ± s.d. (n=6). **C.** Tumor associated fibroblasts were isolated from *Hif-1α*$^{F/F}$ mice bearing Myc-CaP tumors, plated, infected with Ad-Cre or Ad-GFP viruses and cultured under normoxic or hypoxic conditions for 24 hrs. Expression of the indicated mRNAs was quantitated as above. Results are averages ± s.d. (n=6).

Figure 9: A, B. Six weeks old FVB/N male mice (n=10 per group) were castrated or sham operated and their prostates were collected 1 week after surgery. Expression of the indicated inflammatory cytokines, chemokines and cell marker mRNAs was quantitated by Q-PCR and normalized to that of cyclophilin A mRNA. Results are averages ± s.d.. **C.** Six weeks old FVB/N male mice (n=10) were castrated and after 1 week their prostates were collected and stained with CXCL13, B220 and α-SMA antibodies and examined by indirect immunofluorescence (Magnification: 200X). **D, E.** Twelve weeks old TRAMP mice (n=10) were castrated or sham operated and their tumors were collected at the indicated times after castration. Total RNA was extracted and expression of the indicated mRNAs was quantified by Q-PCR and normalized to that of cyclophilin A mRNA Results are averages ± s.d.. (D). Tumors were fixed, paraffin embedded, sectioned and analyzed for α-SMA expression by IHC (Magnification: 200X) (E). **F.** Six weeks old TRAMP males (n=10 per group) were vaccinated three times with 10^8 CFU of TOPO or FAP vaccines every 5 days, followed by a booster shot every 30 days. Mice were castrated when 12 weeks old and tumor weight was measured after 7 weeks. Results are averages ± s.d..

Figure 10: **A.** TRAMP mice (n=10 per group) were vaccinated with TOPO or FAP vaccines as described in Figure 9F, sham operated or castrated when 12 weeks old and tumors were collected 7 weeks later and analyzed for α-SMA expression by Q-PCR. Results are averages ± s.d.. **B.** Tumors were established, collected and processed as in A and analyzed for α-SMA expression by IHC at C7 (Magnification: 200x). **C.** The same tumors collected in B were also analyzed by TUNEL staining (Magnification: 200x).

Figure 11: A-C. Paraffin embedded human prostate tissues (normal, benign hyperplasia and malignant) were sectioned and stained for FAP and SMAD2/3 (A), FAP and CXCL13 (B) and FAP and HIF-1α (C) by IHC (Magnification: 200X). Higher magnification images (400X) are also included. **D.** Frozen sections were from sub-cutaneous xenograft tumors that arose from a primary patient surgical bone metastasis PC specimen. The primary patient tumor was minced to 1 mm pieces, mixed 1:1 in matrigel and 0.1 ml vol/vol implanted sub-cutaneously into 6 weeks old *Rag2*$^{-/-}$;*γc*$^{-/-}$ male mice. Tumors were harvested after 11 weeks. Frozen sections were stained for CXCL13 and FAP by IHC (Magnification: 200X).

Figure 1

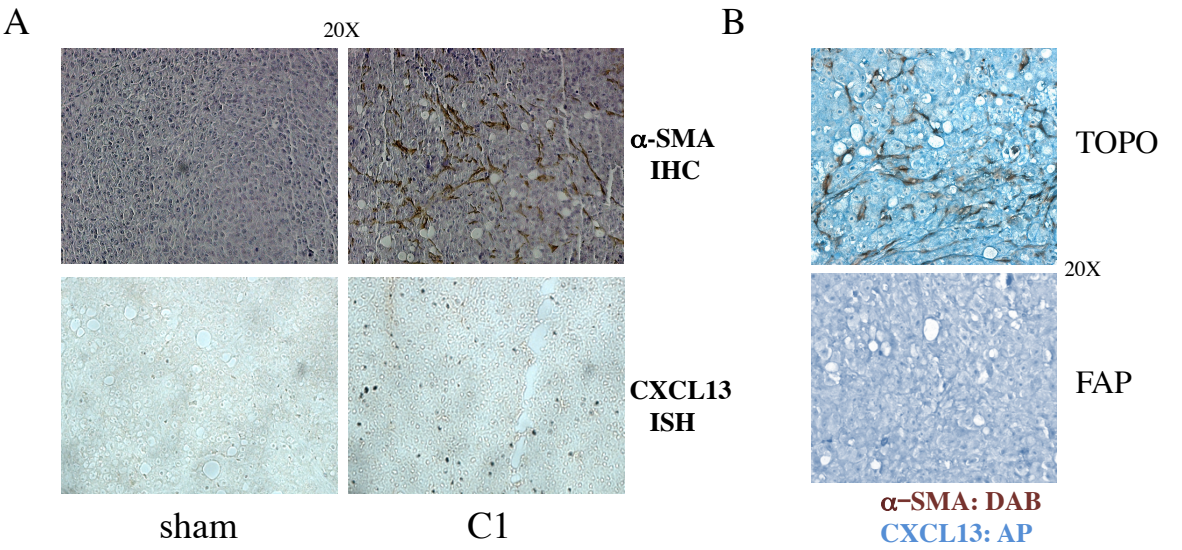
A
20X
α-SMA IHC
CXCL13 ISH
sham
C1
B
TOPO
20X
FAP
α−SMA: DAB
CXCL13: AP

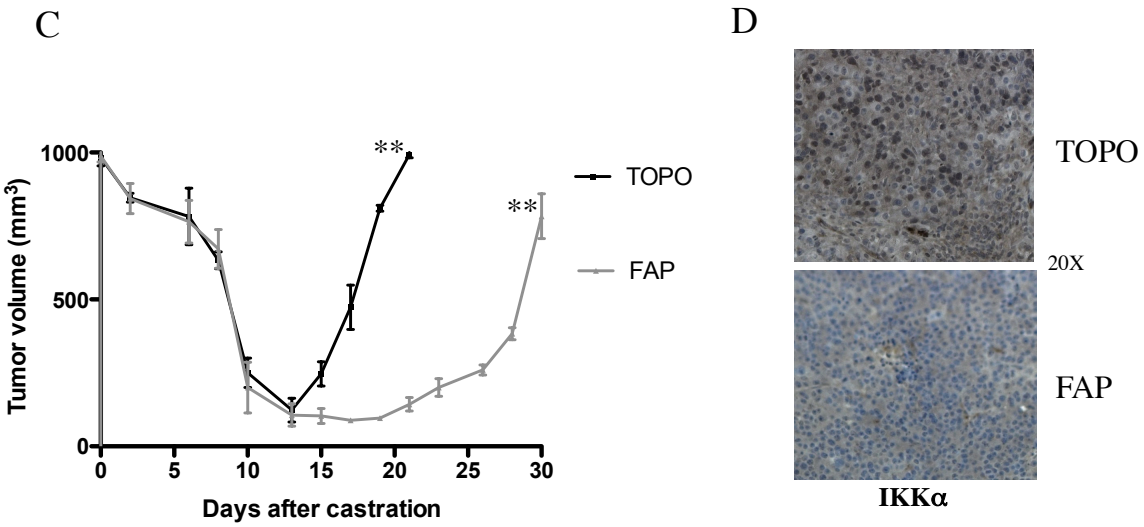
C
Tumor volume (mm³)
1000
500
0
0
5
10
15
20
25
30
Days after castration
**
**
TOPO
FAP
D
TOPO
20X
FAP
IKKα

Figure 2

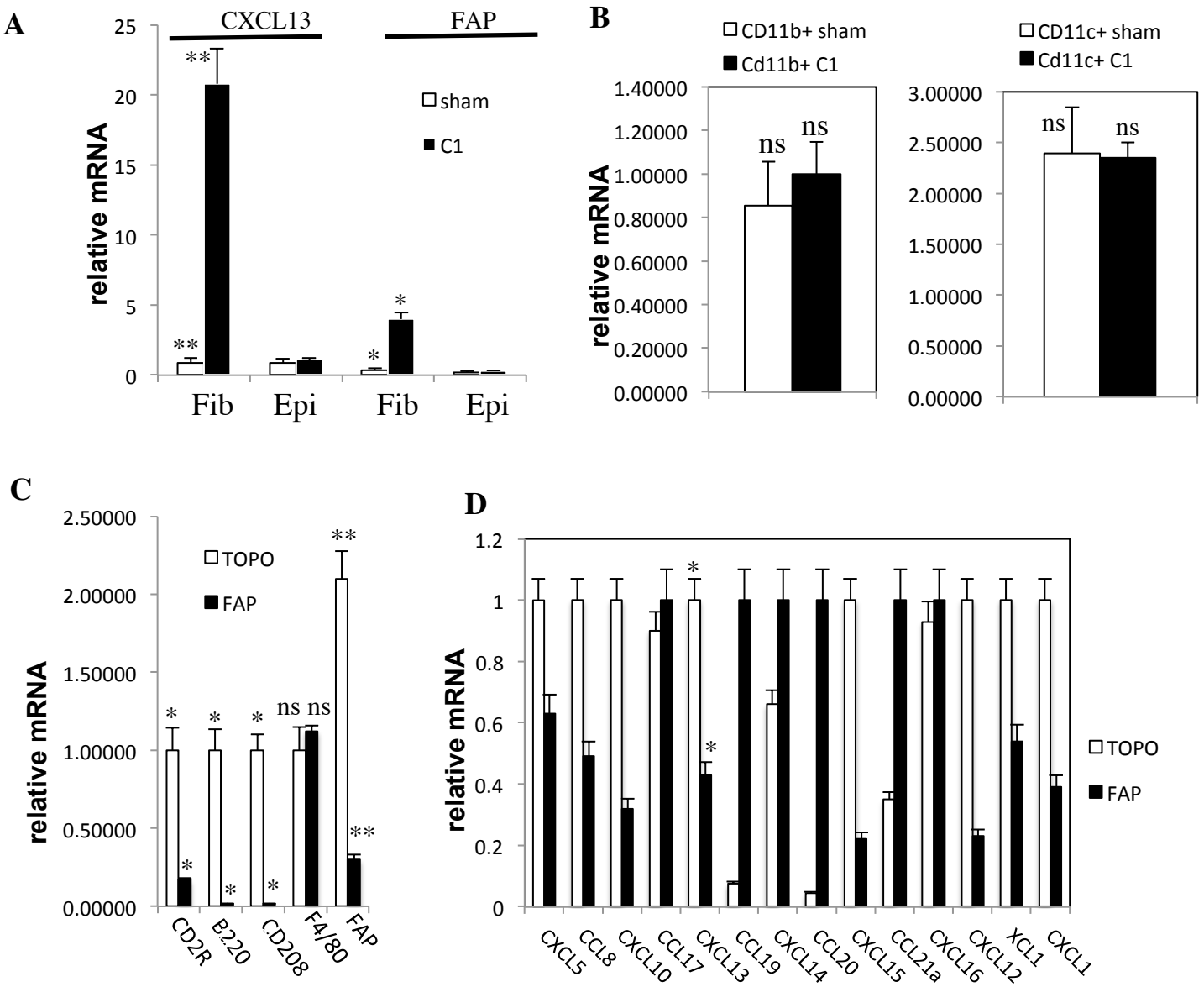
A
CXCL13
FAP
sham
C1
relative mRNA
Fib
Epi
Fib
Epi
B
CD11b+ sham
Cd11b+ C1
CD11c+ sham
Cd11c+ C1
relative mRNA
ns
C
TOPO
FAP
relative mRNA
CD2R
B220
CD208
F4/80
FAP
D
TOPO
FAP
relative mRNA
CXCL5
CCL8
CXCL10
CCL17
CXCL13
CCL19
CXCL14
CCL20
CXCL15
CCL21a
CXCL16
CXCL12
XCL1
CXCL1

Figure 3

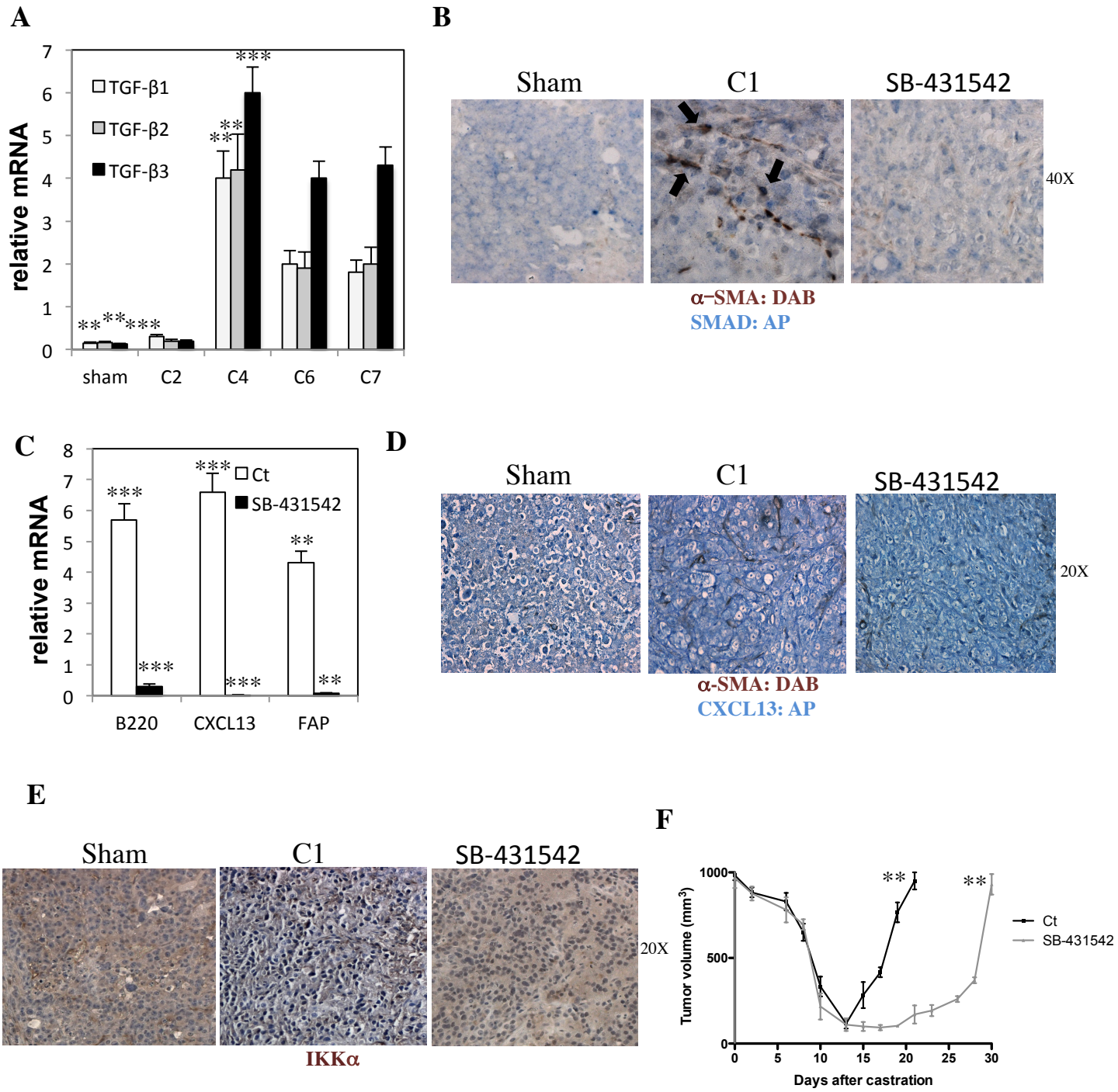
A
relative mRNA
TGF-β1
TGF-β2
TGF-β3
sham
C2
C4
C6
C7
B
Sham
C1
SB-431542
40X
α–SMA: DAB
SMAD: AP
C
relative mRNA
Ct
SB-431542
B220
CXCL13
FAP
D
Sham
C1
SB-431542
20X
α-SMA: DAB
CXCL13: AP
E
Sham
C1
SB-431542
20X
IKKα
F
Tumor volume (mm3)
Days after castration
Ct
SB-431542

Figure 4

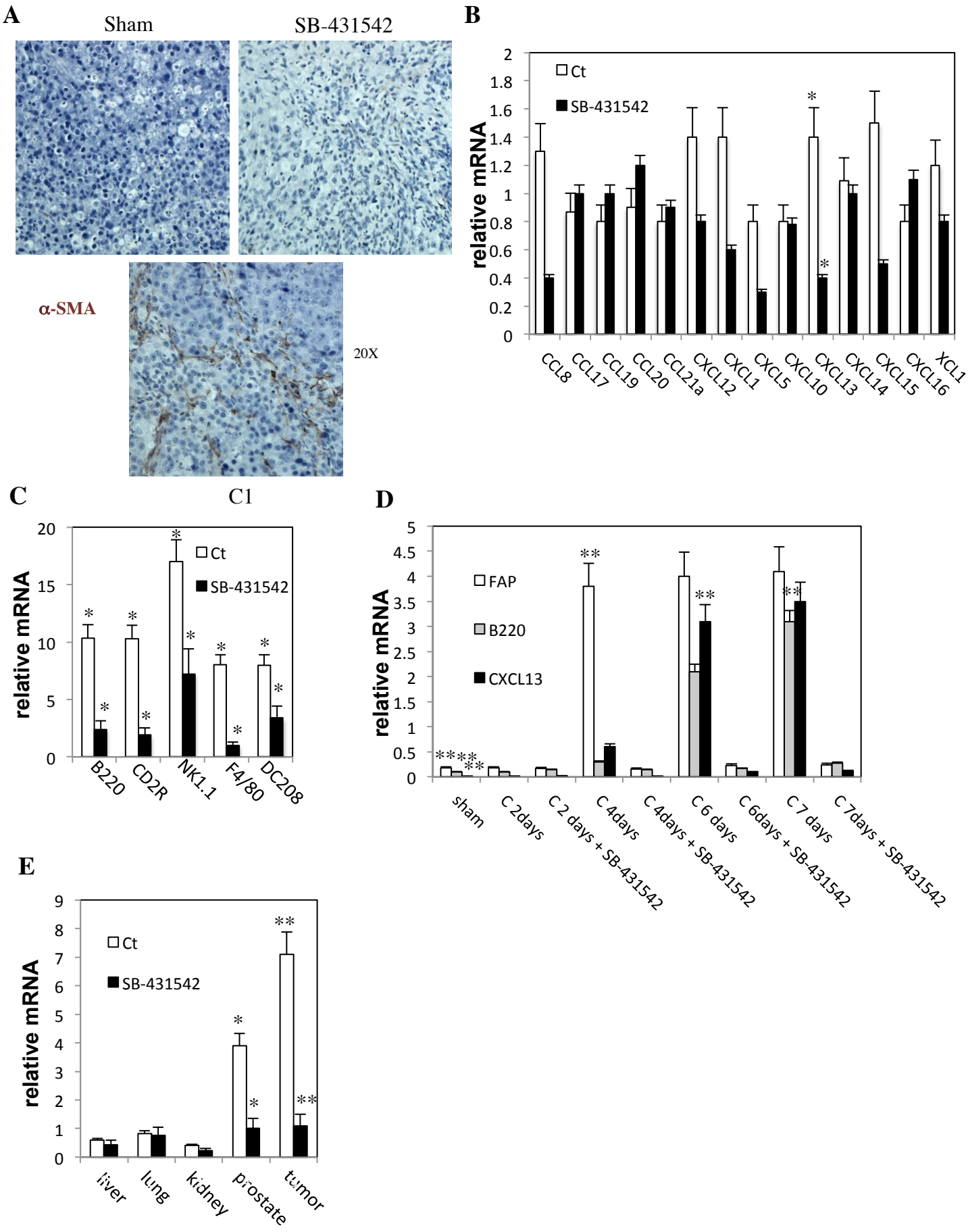
A
Sham
SB-431542
α-SMA
20X
B
Ct
SB-431542
relative mRNA
CCL8
CCL17
CCL19
CCL20
CCL21a
CXCL12
CXCL1
CXCL5
CXCL10
CXCL13
CXCL14
CXCL15
CXCL16
XCL1
C
C1
Ct
SB-431542
relative mRNA
B220
CD2R
NK1.1
F4/80
DC208
D
FAP
B220
CXCL13
relative mRNA
sham
C 2days
C 2 days + SB-431542
C 4days
C 4days + SB-431542
C 6 days
C 6days + SB-431542
C 7 days
C 7days + SB-431542
E
Ct
SB-431542
relative mRNA
liver
lung
kidney
prostate
tumor

Figure 5

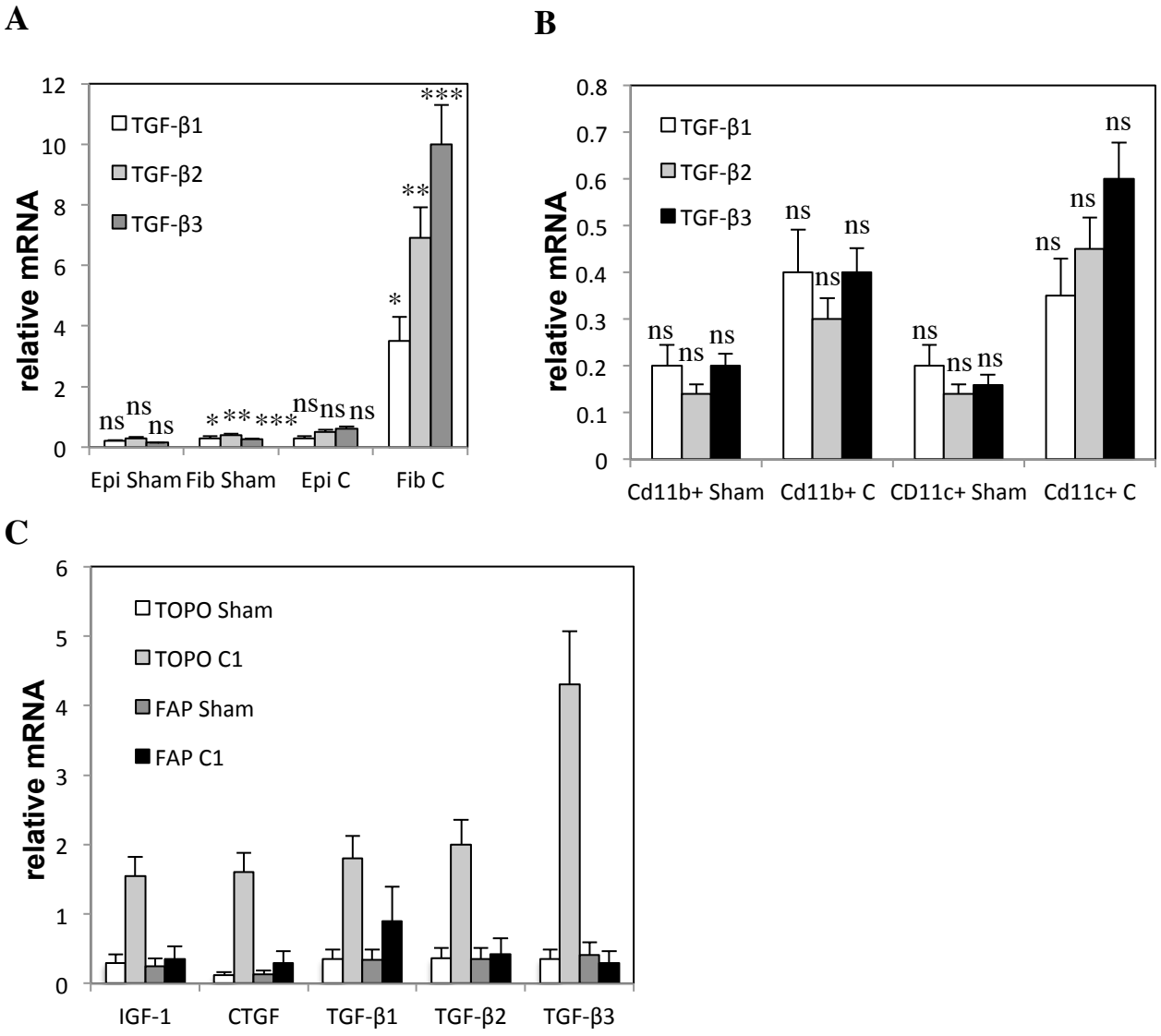
A
relative mRNA
TGF-β1
TGF-β2
TGF-β3
Epi Sham
Fib Sham
Epi C
Fib C
B
relative mRNA
Cd11b+ Sham
Cd11b+ C
CD11c+ Sham
Cd11c+ C
C
relative mRNA
TOPO Sham
TOPO C1
FAP Sham
FAP C1
IGF-1
CTGF
TGF-β1
TGF-β2
TGF-β3

Figure 6

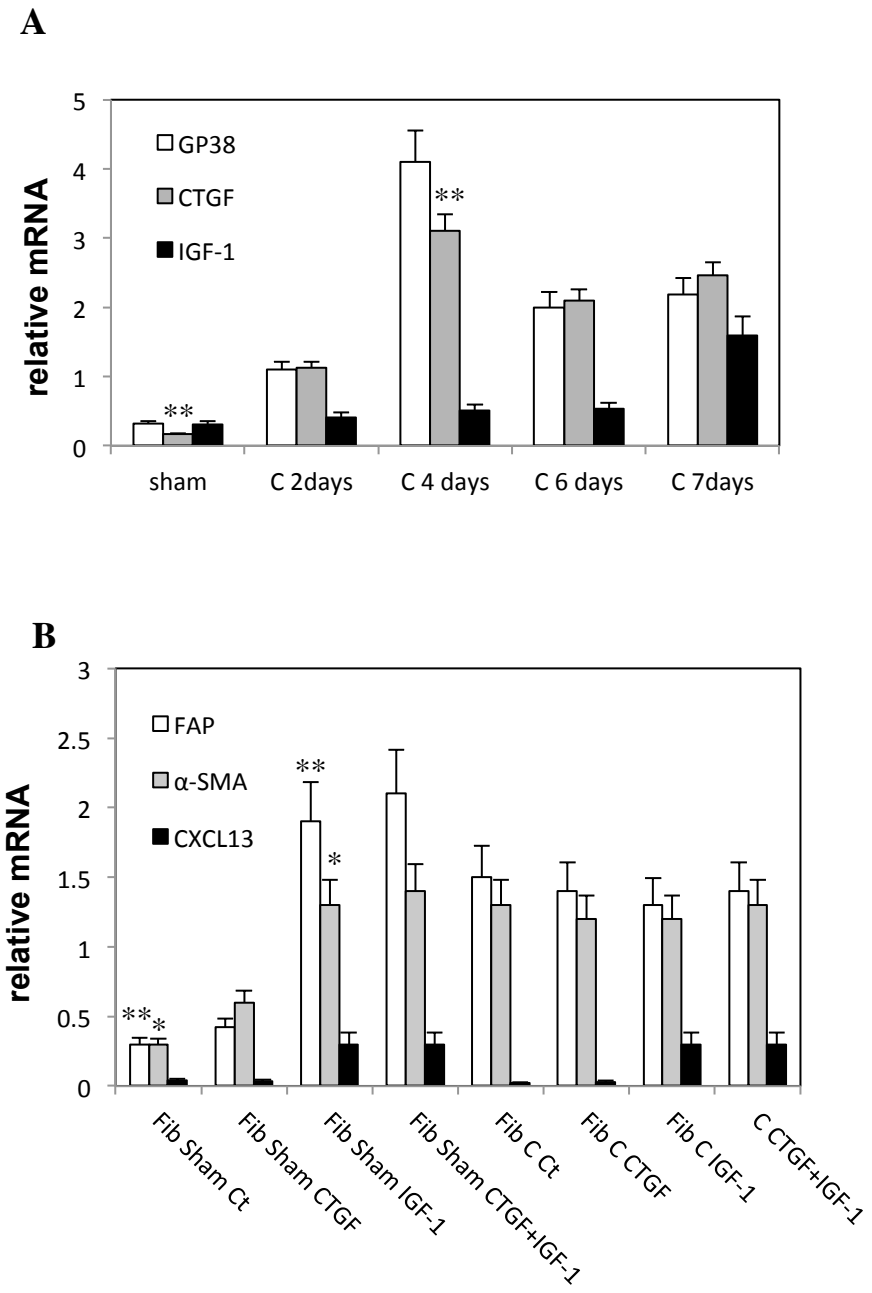
A
relative mRNA
GP38
CTGF
IGF-1
**
sham
C 2days
C 4 days
C 6 days
C 7days
B
relative mRNA
FAP
α-SMA
CXCL13
**
*
Fib Sham Ct
Fib Sham CTGF
Fib Sham IGF-1
Fib Sham CTGF+IGF-1
Fib C Ct
Fib C CTGF
Fib C IGF-1
C CTGF+IGF-1

Figure 7

A

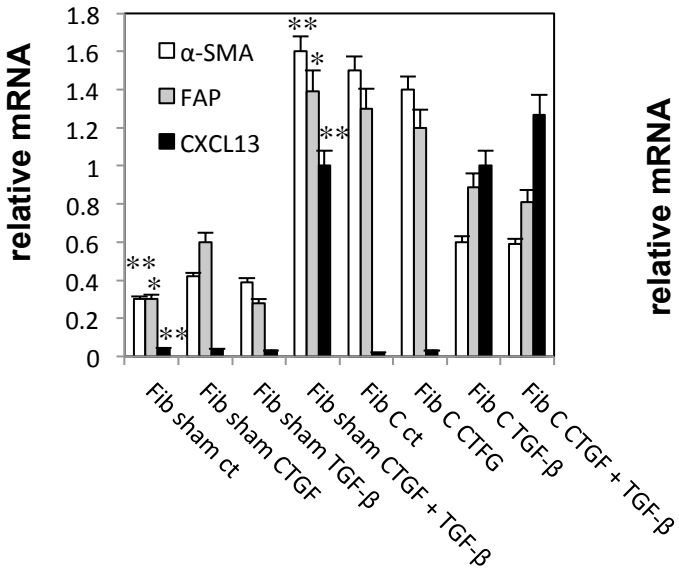
relative mRNA
1.8
1.6
1.4
1.2
1
0.8
0.6
0.4
0.2
0
α-SMA
FAP
CXCL13
Fib sham ct
Fib sham CTGF
Fib sham TGF-β
Fib sham CTGF + TGF-β
Fib C ct
Fib C CTFG
Fib C TGF-β
Fib C CTGF + TGF-β

B

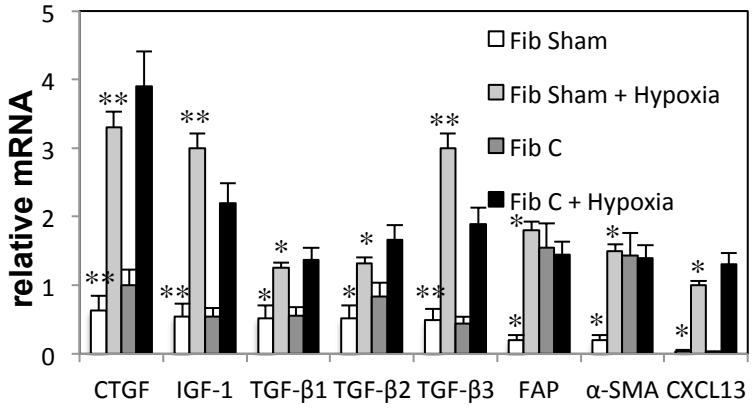
relative mRNA
5
4
3
2
1
0
Fib Sham
Fib Sham + Hypoxia
Fib C
Fib C + Hypoxia
CTGF
IGF-1
TGF-β1
TGF-β2
TGF-β3
FAP
α-SMA
CXCL13

C

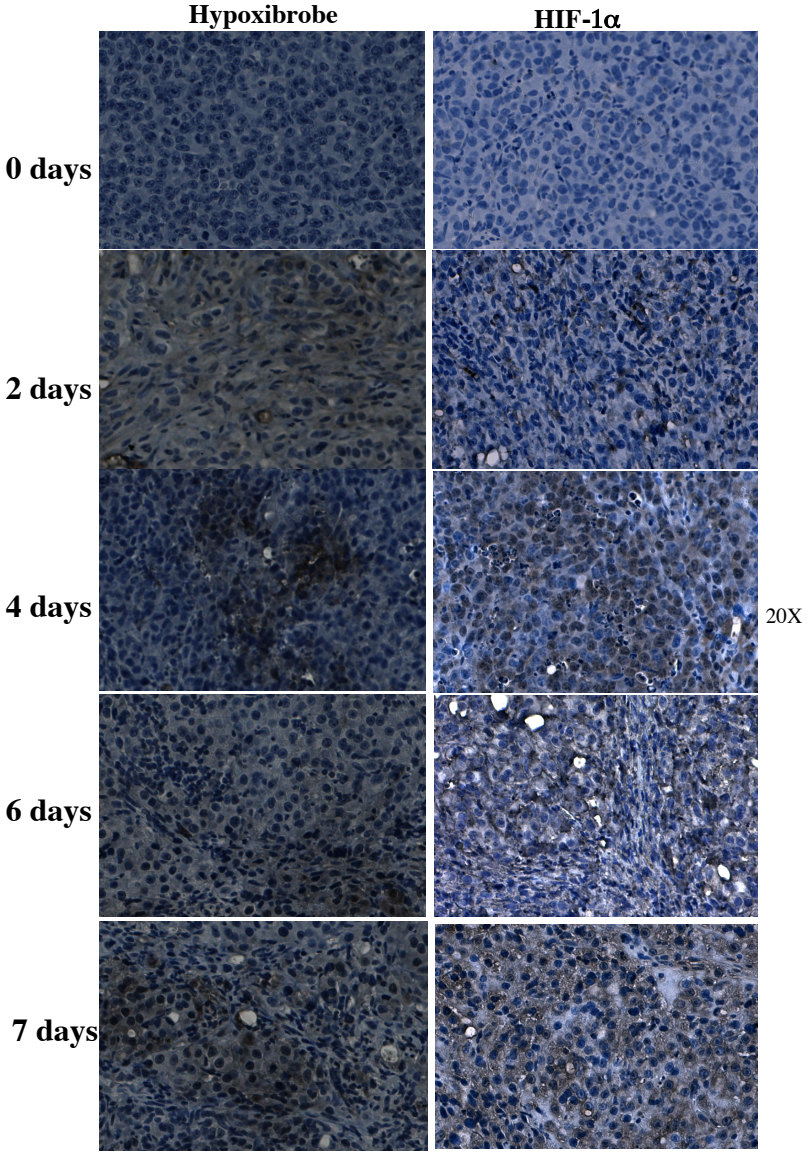
Hypoxibrobe
HIF-1α
0 days
2 days
4 days
6 days
7 days
20X

Figure 8

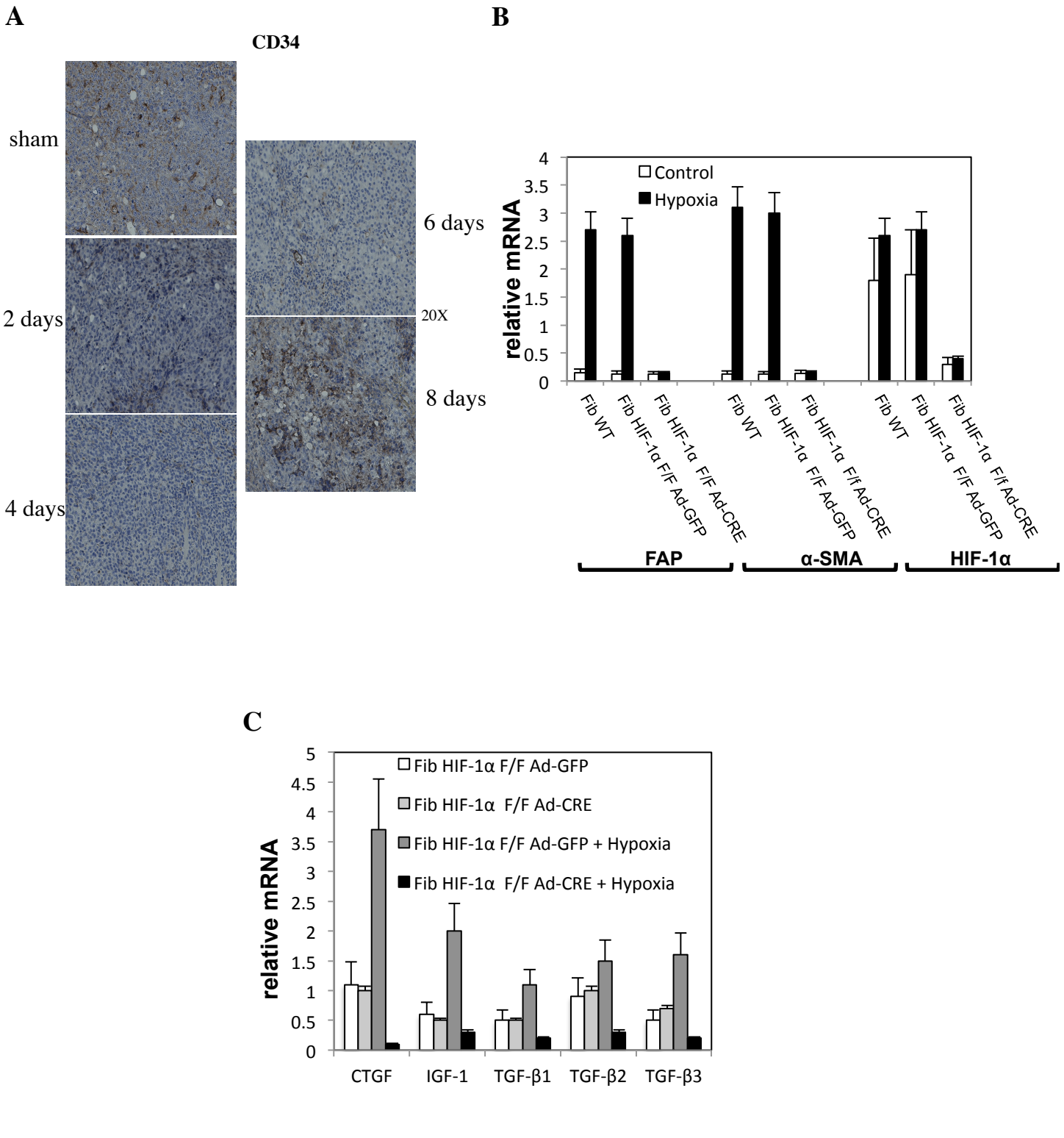
A
CD34
sham
2 days
4 days
6 days
8 days
20X
B
relative mRNA
Control
Hypoxia
Fib WT
Fib HIF-1α F/F Ad-GFP
Fib HIF-1α F/F Ad-CRE
Fib WT
Fib HIF-1α F/F Ad-GFP
Fib HIF-1α F/f Ad-CRE
Fib WT
Fib HIF-1α F/F Ad-GFP
Fib HIF-1α F/f Ad-CRE
FAP
α-SMA
HIF-1α
C
relative mRNA
Fib HIF-1α F/F Ad-GFP
Fib HIF-1α F/F Ad-CRE
Fib HIF-1α F/F Ad-GFP + Hypoxia
Fib HIF-1α F/F Ad-CRE + Hypoxia
CTGF
IGF-1
TGF-β1
TGF-β2
TGF-β3

Figure 9

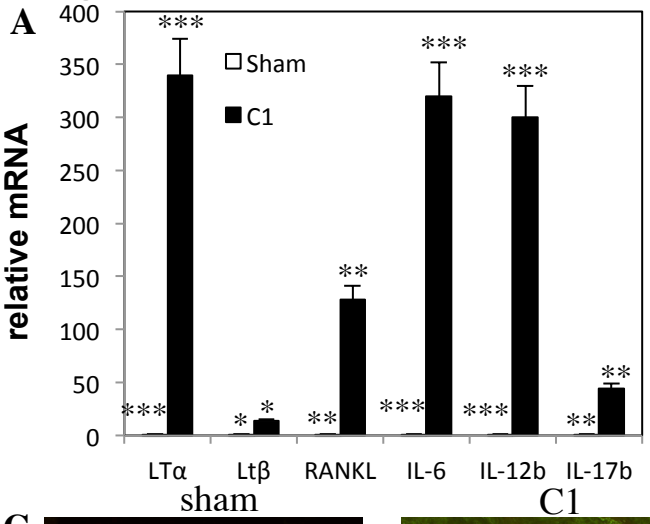
A
relative mRNA
Sham
C1
LTα
Ltβ
RANKL
IL-6
IL-12b
IL-17b

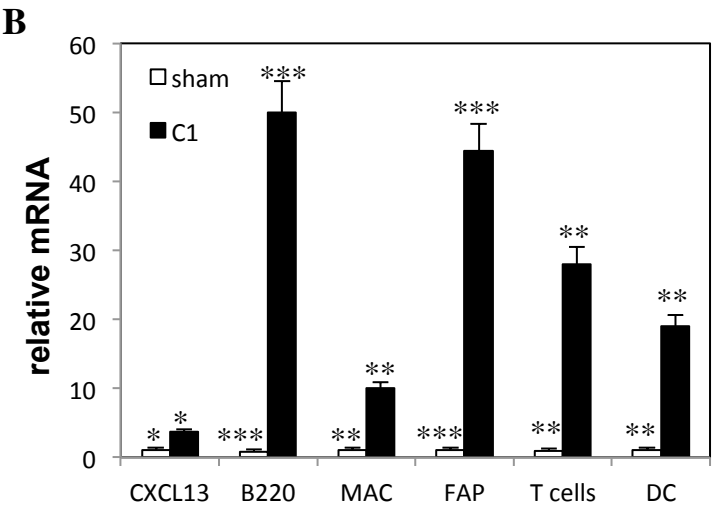
B
relative mRNA
sham
C1
CXCL13
B220
MAC
FAP
T cells
DC

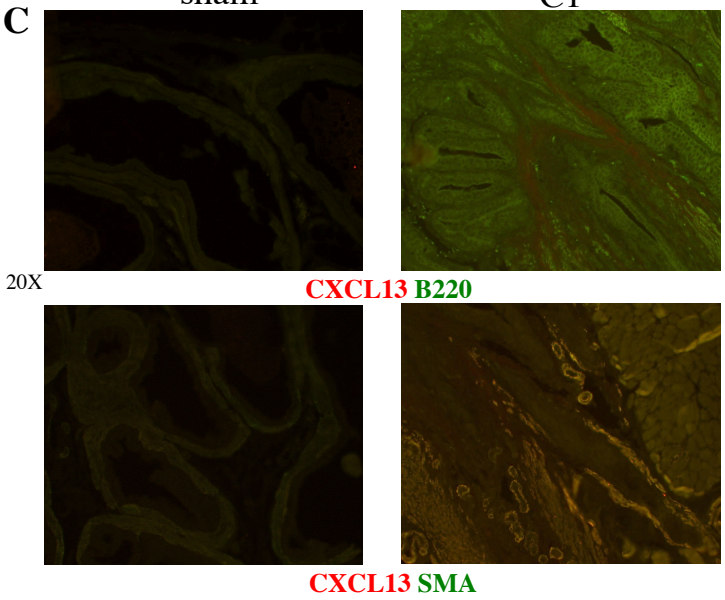
C
sham
C1
20X
CXCL13 B220
CXCL13 SMA

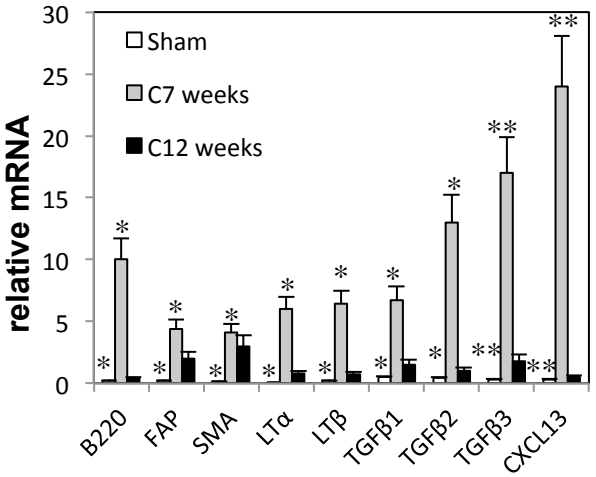
D
relative mRNA
Sham
C7 weeks
C12 weeks
B220
FAP
SMA
LTα
LTβ
TGFβ1
TGFβ2
TGFβ3
CXCL13

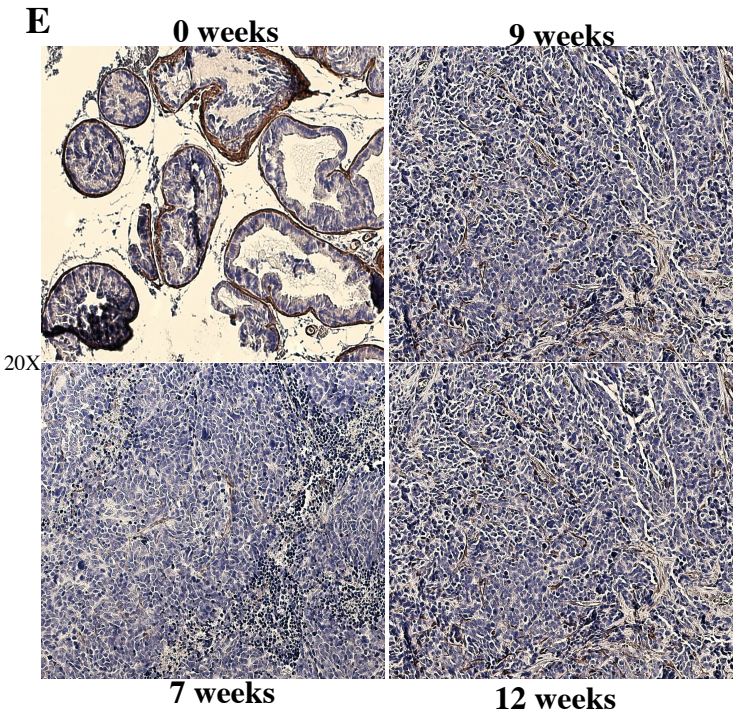
E
0 weeks
9 weeks
20X
7 weeks
12 weeks

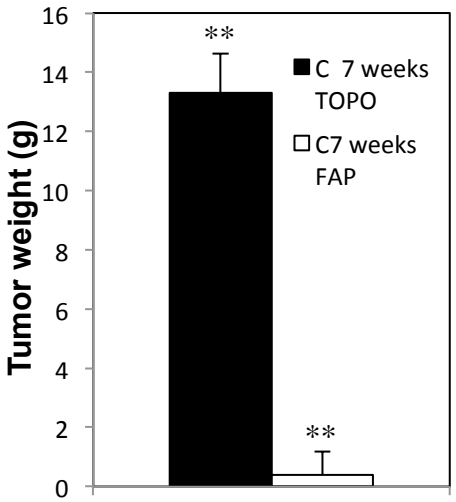
F
Tumor weight (g)
C 7 weeks TOPO
C7 weeks FAP

Figure 10

A

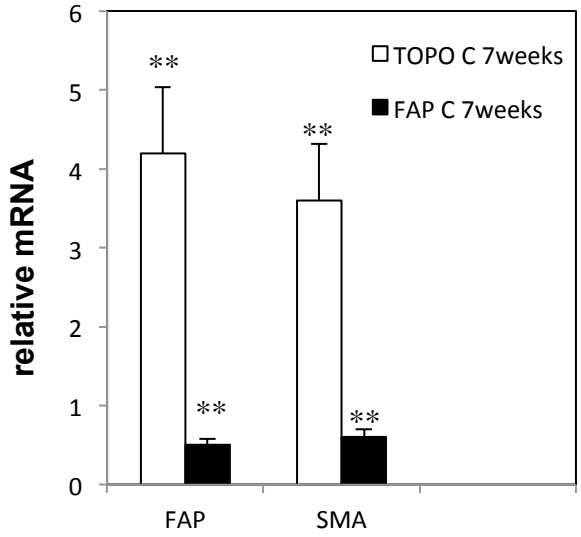

B

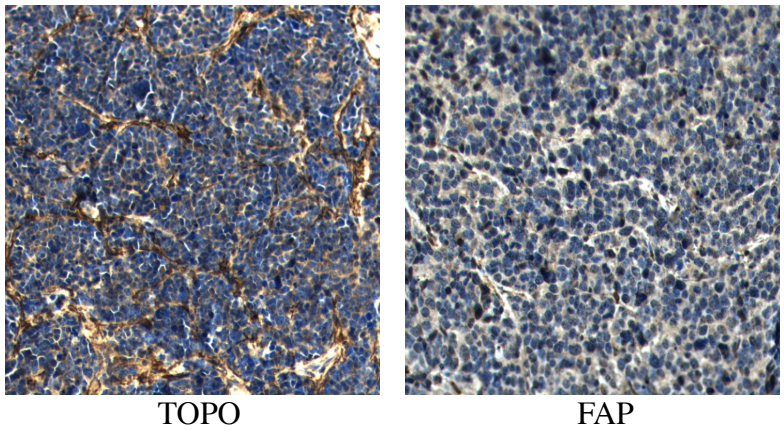

C

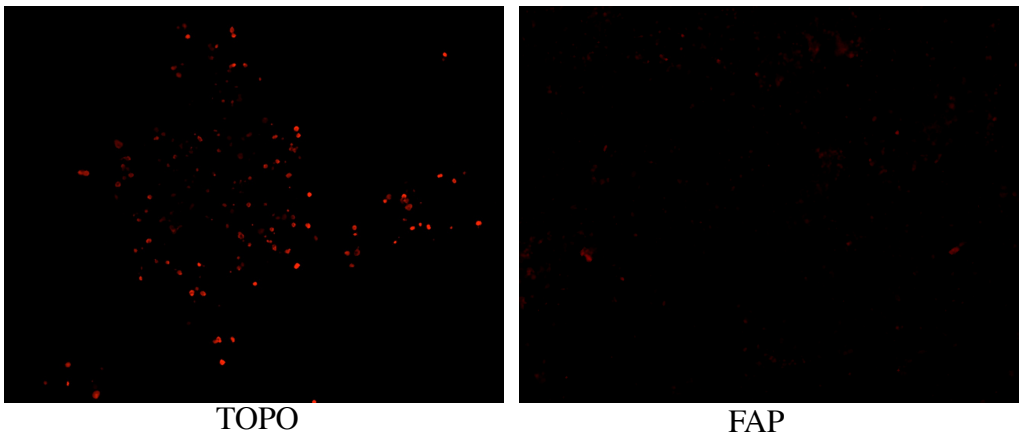

Figure 11

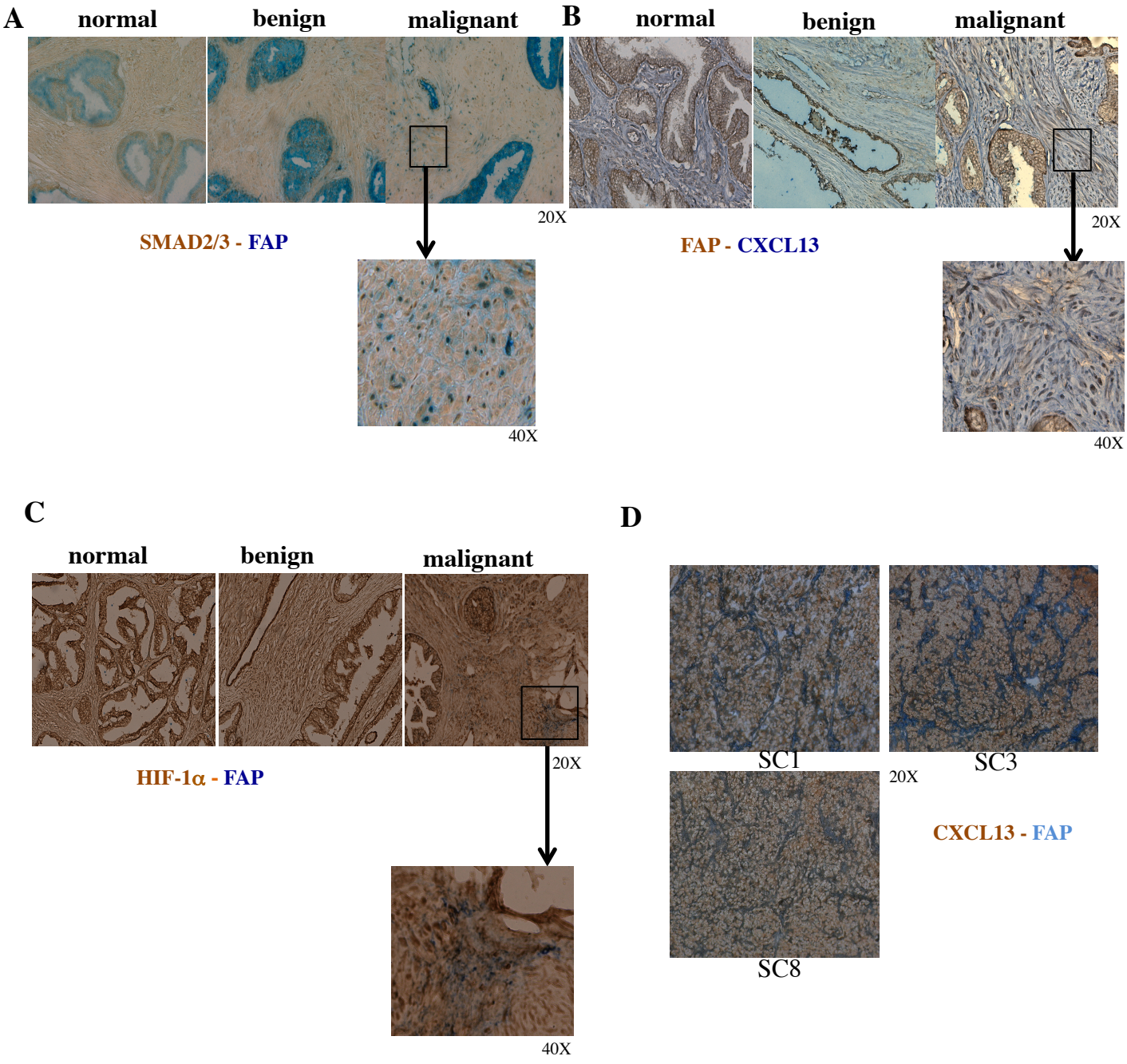
A
normal
benign
malignant
20X
SMAD2/3 - FAP
40X
B
normal
benign
malignant
20X
FAP - CXCL13
40X
C
normal
benign
malignant
20X
HIF-1α - FAP
40X
D
SC1
SC3
20X
CXCL13 - FAP
SC8